analytical chemistry

pubs.acs.org/ac Article

Nondestructive Analysis of Mummification Balms in Ancient Egypt Based on EPR of Vanadyl and Organic Radical Markers of Bitumen

Charles E. Dutoit,* Laurent Binet, Hitomi Fujii, Agnes Lattuati-Derieux, and Didier Gourier*

Cite This: https://dx.doi.org/10.1021/acs.analchem.0c03116 Read Online

ACCESS | Metrics & More | Article Recommendations | Supporting Information

ABSTRACT: The black matter employed in the funeral context by ancient Egyptians is a complex mixture of plant-based compounds with variable amounts of bitumen. Asphaltene, the most resistant component of bitumen, contains vanadyl porphyrins and carbonaceous radicals, which can be used as paramagnetic probes to investigate embalming materials without sample preparation. Electron paramagnetic resonance (EPR) at the X-band, combining in-phase and out-of-phase detection schemes, provides new information in a nondestructive way about the presence, the origin, and the evolution of bitumen in these complex materials. It is found that the relative EPR intensity of radicals and vanadyl porphyrins is sensitive to the origin of the bitumen. The presence of nonporphyrinic vanadyl complexes in historical samples is likely due to the complexation of VO^{2+} ions by carboxylic functions at the interface between bitumen and other biological components of the embalming matter. The absence of such oxygenated vanadyl complex in natural bitumen and in one case of historical human mummy acquired by a museum in the 19th century reveals a possible, nondocumented, ancient restoration of this mummy by pure bitumen. The linear correlation between in-phase and out-of-phase EPR intensities of radicals and vanadyl porphyrins in balms and in natural bitumen reveals a nanostructuration of radicals and vanadyl porphyrin complexes, which was not affected by the preparation of the balm. This points to the remarkable chemical stability of paramagnetic probes in historical bitumen in ancient Egypt.

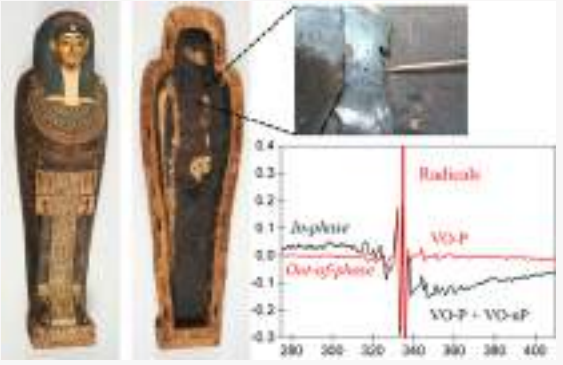

Downloaded via SAN FRANCISCO STATE UNIV on November 18, 2020 at 00:54:56 (UTC).
See https://pubs.acs.org/sharingguidelines for options on how to legitimately share published articles.

Embalming matter and other "black matter" used in ancient Egypt are complex mixtures of natural compounds such as sugar gum, beeswax, fats, coniferous resins, bitumen, and so on.[1−3] Each of these substances is characterized by specific molecular biomarkers identified by various methods of analytical organic chemistry, among which gas chromatography−mass spectrometry (GC/MS) and pyrolysis−gas chromatography−mass spectrometry (Py−GC/MS) are the most commonly used. Since the 19th century, and in spite of many controversies, egyptologists have believed that the dark color of mummies is due to the presence of bitumen.[4−8] Based on specific molecular biomarkers, mainly hopanes and steranes, and on radiocarbon analysis (bitumen has lost its ^{14}C), it was concluded that bitumen was increasingly used for mummification receipts from the New Kingdom (ca 1550−1070 BC) to the Ptolemaic/Roman period (332 BC- IVth century AC).[3] Although the ensemble of destructive organic analytical and radiocarbon methods used so far is powerful to study separately the many pieces of the puzzle, there does not seem to be a method for analyzing the whole puzzle, i.e., in a nondestructive manner. This is understandable given the extreme chemical complexity of these embalming materials, which necessitates preparation and separation steps prior to a detailed molecular or isotopic analysis. A complementary, but different, method could be used to analyze these materials "from the inside" using internal probes already present in very small quantities but which would provide information on their environment. It is well known that oil, kerogens, and bitumen contain variable amounts of vanadyl porphyrins (up to 1000 ppm), which originate from photosynthetic life in a primitive marine environment (which provide porphyrinic molecules). Vanadyl porphyrins are formed by substitution of Mg^{2+} ions of chlorophyll by VO^{2+} ions during diagenesis.[9] Carbonaceous radicals are also formed during the geological evolution of the fossil biological matter.[10−12] Vanadyl porphyrin complexes and carbonaceous radicals are mainly located in the asphaltene component of the bitumen, a tridimensional polymerized architecture that is resistant to biodegradation and oxidation.[13] In this work, using electron paramagnetic resonance (EPR) spectroscopy, we explore the possibility of analyzing the vanadyl complexes and organic radicals in historical samples of black matter taken from historical human and animal Egyptian

Received: July 22, 2020
Accepted: November 4, 2020

© XXXX American Chemical Society

https://dx.doi.org/10.1021/acs.analchem.0c03116
Anal. Chem. XXXX, XXX, XXX−XXX

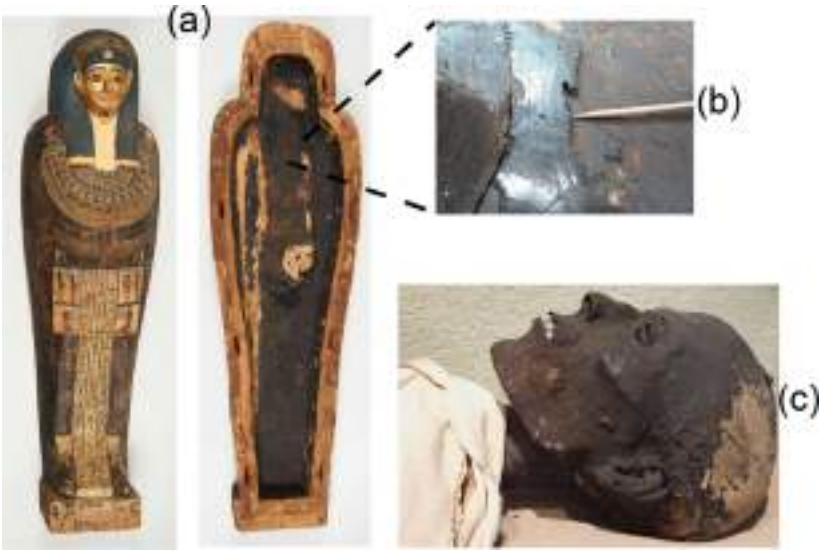

Figure 1. Two examples of samples of black matter studied in this work: (a) Coffin of Irethorerou (Ptolemaïc Period), Musée d'Art et d'Histoire, Narbonne, France and (b) black matter at the bottom of the coffin from which the sample ***Hum 1*** was taken, reproduced with permission from C2RMF/Anne Chauvet [Copyright 2020]. (c) Head of the mummy of a bearded man (Late Period), Chateau-musée, Boulogne-sur-Mer, France. Sample ***Hum 3*** was taken from the mummy's neck, reproduced with permission from Frédérique Vincent [Copyright 2020].

mummies. The main objective is to use these stable paramagnetic probes to obtain information on the presence, origin, processing, and evolution of bitumen in embalming matter. These data are faced with molecular characterization obtained from a classical GC/MS approach.

EXPERIMENTAL SECTION

Samples. The samples of black matter studied in this work come from various human and animal mummies of ancient Egypt stored in museum collections. They were compared with three reference samples: a natural asphalt from the Dead Sea (***Ref 1***), a commercial bitumen of Judea (***Ref 2***), and a bitumen from the tar seep of the Puy de la Poix, Clermont-Ferrand, France (***TS***). Three samples of black matter were taken from an anthropomorphic coffin (***Hum 1***) and two human mummies (***Hum 2*** and ***Hum 3***) (Figure 1). Four samples were taken from animal mummies: three rams (***An 1***, ***An 2***, ***An 3***) and one crocodile (***An 4***). All of these samples date from the Late Period to the Ptolemaic Period (744−30 BC). All samples (10−20 mg) were inserted into quartz Suprasil EPR tubes. The characteristics of the samples are summarized in Table 1 and described in detail in Supporting Information Table S1.

Electron Paramagnetic Resonance (EPR). Continuous-wave electron paramagnetic resonance (cw-EPR) measurements were performed at room temperature using a conventional Bruker X-band Bruker Elexsys E500 spectrometer operating at about 9.6 GHz, equipped with a high-sensitivity 4122SHQE/0111 microwave cavity. The microwave power into the cavity was set at 2 mW to avoid saturation of the EPR spectrum. The modulation frequency and modulation depth of the static magnetic field were chosen as 100 kHz and 0.5 mT, respectively. Simulation of cw-EPR spectra was done with the EasySpin package for MATLAB.[14] The g-factors and the hyperfine interaction were fit manually to achieve good similitude between experimental and simulated spectra. Complementary separative and molecular analyses were performed on ***Hum 1*** and ***Hum 3*** samples using GC/MS (see the Supporting Information). These analyses were aimed to identify a large range of natural substances (e.g., fats, waxes, terpenoid resins, and bitumen) that could be possibly present in the selected samples (Figure 1.

Table 1. Samples of Black Matter Studied by EPR

label	object
Ref 1	natural asphalt with VO^{2+}, from the Dead Sea
Ref 2	commercial bitumen of Judea
TS	natural bitumen with no VO^{2+}, France
Hum 1	anthropomorphic coffin, upper Egypt, Ptolemaïc Period (332−30 BC); black matter in the bottom of the coffin
Hum 2	human mummy, Egypt, Late Period (end of the IVth century BC); dark matter covering the mummy
Hum 3	human mummy, Egypt, Late Period (XXIth−XXVth dynasty?); black matter taken from the neck of the mummy
An 1	ram mummy, upper Egypt, Late Period; 672−322 BC; black matter covering the mummy
An 2	ram mummy, upper Egypt, Late Period (664−332 BC); black matter covering the mummy
An 3	ram mummy (the same as ***An 2***); tissue with brown matter covering the mummy
An 4	crocodile mummy, upper Egypt, Ptolemaïc Period; black matter covering the skull

RESULTS AND DISCUSSION

Continuous-Wave EPR Spectroscopy. The EPR spectrum at the X-band of the Dead Sea asphalt sample (***Ref 1***) exhibits the two paramagnetic species classically found in bitumen and oil (Figure 3a):[10,15−17] (i) a single and intense line in the central part of the spectrum (~335 mT, g = 1.9994, line width ΔB = 0.44 ± 0.08 to 0.52 ± 0.08 mT), corresponding to free organic radicals (S = 1/2), hereafter referred to as C^0, and (ii) a multiline spectrum of vanadyl porphyrins in asphaltene, hereafter referred to as VO-P. The shape of this spectrum is dominated by the central VO^{2+} ion of VO-P (Figure 2), which bears an unpaired electron spin S = 1/2 in the d_{xy} orbital of V^{4+} ($3d^1$ configuration) in the porphyrin plane, with lobes pointing between N atoms of pyrrolic groups. The hyperfine interaction of the electron spin S with the nuclear spin I = 7/2 of the central ^{51}V nucleus (100%

https://dx.doi.org/10.1021/acs.analchem.0c03116
Anal. Chem. XXXX, XXX, XXX−XXX

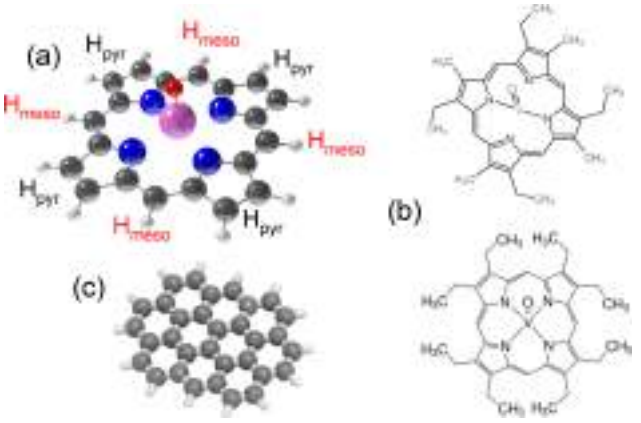

Figure 2. (a) Chemical structure of a VO porphyrin model; (b) top: VO-etioporphyrin (VOEtio) and bottom: VO-octaethyl porphyrin (VOOEP), among the most common geoporphyrins; and (c) schematic representation of a polyaromatic radical.

abundance) gives two sets of $2I + 1 = 8$ hyperfine lines. The most extended and weaker set of lines, characterized by parameters $g_{//}$ and $A_{//}$, corresponds to VO-P complexes with the V−O bond oriented along the external field $\mathbf{B}_0$. The most intense central set of eight lines, with parameters $g_\perp$ and $A_\perp$, corresponds to complexes with $\mathbf{B}_0$ in the porphyrin plane (perpendicular to the VO bond). The bitumen of Judea (***Ref 2***) gives the same EPR spectrum (see Figure S1a in the Supporting Information).

EPR spectra of historical samples of black matter exhibit the same general pattern, as exemplified in Figure 3b for the Ptolemaïc coffin (***Hum 1***). The other spectra are given in the Supporting Information. Except for the ***Hum 3*** sample (the bearded man from the Boulogne museum, Figures 1c and S1b), all of the historical samples exhibit distinct EPR features (Figures 3, S1, and S2): (i) a VO-P spectrum less intense than in reference samples for the same mass of matter, (ii) additional hyperfine lines, marked by green circles in Figure 3b, and (iii) a very broad line covering all of the spectra, due to traces of ferromagnetic mineral particles (iron oxides). The manifestation of the latter is a distortion of the baseline of the VO^{2+} spectrum, and it will not be considered further in this work. The additional hyperfine lines in historical samples are clearly due to a second VO^{2+} species (hereafter referred to as VO-nP), as shown by the simulation of EPR spectra (Figure 3c). The shapes of the hyperfine patterns of VO-P and VO-nP are very similar, except for the resonance field of each hyperfine line, which indicate that the EPR parameters of these two vanadyl complexes are different.

The simulation parameters for each sample are given in Supporting Information Table S2. The mean values of the EPR parameters are given in Table 2, the error bars representing the dispersion of simulated values. It is well known that EPR parameters g and A of V^{4+} are sensitive to the symmetry and the nature of its sphere of coordination,[18] which can be visualized in a diagram representing $g_{//}$ versus $A_{//}$ for the nine samples (Figure 4a). The background of this diagram is built from multiple experimental data collected from the literature for V^{4+} and VO^{2+} in various mineral matrices and vanadyl complexes (ref 19 and references therein). The colored triangle in the lower left part of Figure 4a represents the location of data for V^{4+} in oxide minerals, and the ellipses (solid lines) in the upper right part represent the location of data for vanadyl

Table 2. Mean Values of EPR Parameters of Vanadyl Complexes[a]

complex	$g_{//}$	$g_\perp$	$A_{//}$	$A_\perp$
VO-P	1.957 ± 0.002	1.978 ± 0.002	158 ± 3	55 ± 2
VO-nP	1.925 ± 0.003	1.978 ± 0.003	176 ± 3	70 ± 3

[a]Hyperfine interaction A is given in 10^{-4} cm^{-1}.

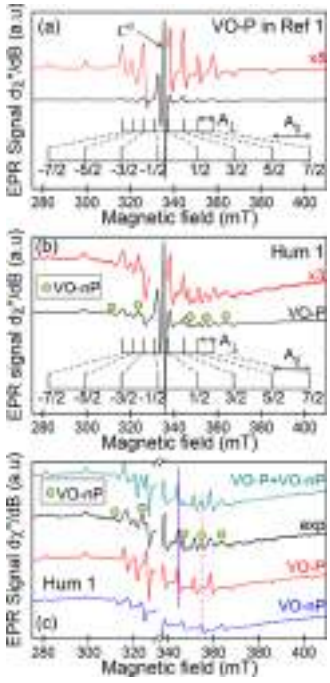

Figure 3. EPR spectra at the X-band and room temperature of two samples of black matter: (a) asphalt from the Dead Sea ***Ref 1*** and (b) black matter in the Ptolemaïc coffin ***Hum 1***; (c) simulation of the EPR spectrum of ***Hum 1***; some EPR lines of VO-nP are represented by green circles.

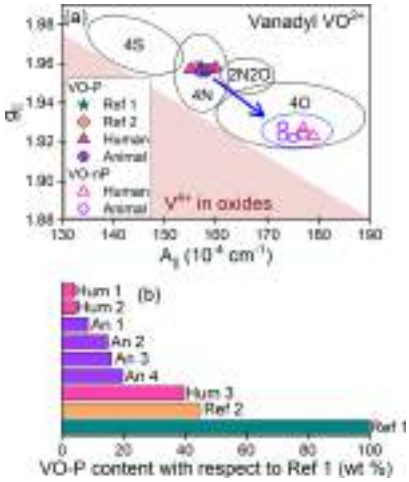

Figure 4. (a) Diagram representing $g_{//}$ versus $A_{//}$ for V^{4+}; the pink triangle in the lower part represents the location of data for V^{4+} ions in oxides; the ellipses represent the cases of VO^{2+} ions with different types of ligands. (b) Histogram of the VO-P content, with respect to the asphalt from the Dead Sea (***Ref 1***).

https://dx.doi.org/10.1021/acs.analchem.0c03116
Anal. Chem. XXXX, XXX, XXX−XXX

complexes with different types of first neighbor atoms (4S, 4N, 2N2O, and 4O). It can be seen that VO-P spectra of all samples (***Ref***, ***Hum***, and ***An***) have four N ligands, as expected for vanadyl porphyrins. VO-nP spectra of historical samples have clearly four oxygenated ligands, which indicates that the VO-nP species found in historical samples are nonporphyrinic vanadyl complexes.

As the black matter used in ancient Egypt was generally a complex mixture of plant-based resins and bitumen (mainly from the Dead Sea),[1−3,20−23] we may compare the amount of VO-P for each sample and for the same sample mass, relative to the Dead Sea asphalt (***Ref 1***) taken as the reference (100% of VO-P). The results are given in Figure 4b. Samples from animal mummies (***An 1−4***) are characterized by almost the same proportion of VO-P (10−20%), while samples of black matter from human mummies or coffin are poorly enriched (∼5% for ***Hum 1*** and ***Hum 2***) or very enriched (40% for ***Hum 3***) in VO-P. The amount of VO-P in sample ***Hum 3*** is very similar to that in the commercial bitumen of Judea ***Ref 2***. In principle, these relative amounts of VO-P could be an indication of the proportion of bitumen in the black matter. However, this would be true only if the bitumen of all samples came from the same region, as the vanadyl content of bitumen is dependent on the geological formation. Even in the case of the floating blocks of Dead Sea asphalt exploited in the antiquity, it has been observed that blocks taken from the northern part of the lake are rich in VO-P, while those taken from the southern part are poor.[10] As the chemical analysis of ***Hum 3*** indicates that it is pure bitumen (see the Supporting Information), we may conclude that this bitumen contains less VO-P than the Dead Sea asphalt of ***Ref 1***.

For this reason, it is necessary to use another marker in addition to the VO-P content of the black matter. The free carbonaceous radicals C^0, responsible for the intense central line of EPR spectra (Figure 3), are ubiquitous in all mature kerogens, even those older than 3 billion years or in carbonaceous meteorites.[24−27] Consequently, the C^0 line is present in all bitumen samples, either of marine origin (with VO-P) or of land-plant origin (without VO-P). The latter case is illustrated with the bitumen from the tar seep of the Puy de la Poix, Clermont-Ferrand, France (sample ***TS***), which exhibits no VO-P signal but an intense C^0 line and additional hyperfine lines due to Mn^{2+} ions (Figure S3). Thus, useful information about the origin and evolution of bitumen in historical samples can be obtained from correlations among the three internal probes VO-P, VO-nP, and C^0.

Figure 5a represents the intensities $I_{VO\text{-}nP}$ versus $I_{VO\text{-}P}$ of the nonporphyrinic and porphyrinic vanadyl complexes, respectively. The intensities, measured from the amplitude of the +5/2⊥ hyperfine line of the VO^{2+} spectrum (see Figure 3b for the identification of this line), are given for the same mass of matter. It can be seen in this diagram that all historical samples, except ***Hum 3***, contain VO-nP complexes in variable amounts, and their data are clustered in the same region of the diagram. The positions of ***Hum 3*** and the commercial bitumen ***Ref 2*** are very close in the diagram, which suggests that ***Hum 3*** is anomalous compared to other historical samples.

This impression is reinforced in an independent diagram representing, for the same mass of matter, the amplitude of the C^0 line versus the amplitude of the −1/2 ⊥ transition of vanadyl porphyrins VO-P (Figure 5b). Considering again the Dead Sea asphalt (***Ref 1***) and the commercial bitumen (***Ref 2***) as reference samples (pure bitumen), all archeological samples

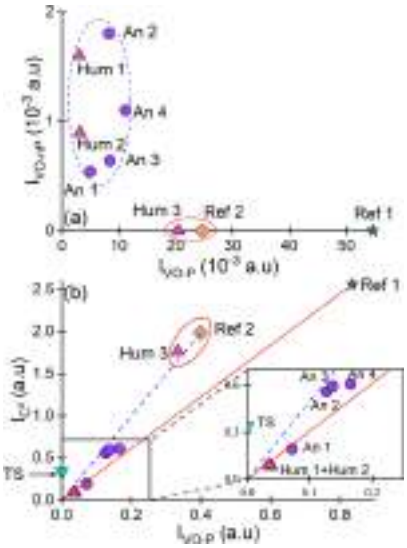

Figure 5. Diagrams representing EPR intensities of VO-P, VO-nP, and C^0 for the same mass of matter: (a) VO-nP versus VO-P and (b) C^0 versus VO-P. The inset represents a zoom of the lower part of the diagram.

are characterized by a ratio $I_C0/I_{VO\text{-}P} \approx 3-5$. The red line and the interrupted blue line in Figure 5b correspond to $I_C0/I_{VO\text{-}P} \approx 3$ and 5, respectively. To obtain more information about the origin of bitumen, we must consider that the black matter in ancient Egypt is a mixture of bitumen with other types of biological matter (plant-based resin, beeswax, animal fat, etc ...). Vanadyl porphyrins VO-P are exclusively localized in bitumen, while, in principle, radicals C^0 may be localized both in bitumen and in the other component so that the intensities $I_{VO\text{-}P}$ and I_C0 can be written as

$$I_{VO-P} = k_1[\text{Bitumen}]$$
$$I_{C^0} = k_2[\text{Bitumen}] + k_3[\text{Other}]$$
$$1 = [\text{Bitumen}] + [\text{Other}] \quad (1)$$

where [Bitumen] and [Other] represent the relative mass content of bitumen and biological material in the black matter. Coefficients k_i (i = 1, 2, 3) depend on several factors, such as the geological context and setting of the bitumen, the composition of the other component of the black matter, or the chemical and physical treatments used for the preparation of the embalming mixture. In particular, although most bitumen samples of marine origin contain significant amounts of VO-P complexes, bitumen from terrestrial plant origin does not contain these complexes or only a very small amount.[10] Hence, k_1 can have a wide range of values, including zero (no VO-P). This is the case for reference sample ***TS*** (Figure S3). On the contrary, bitumen always contains carbonaceous radicals C^0, which originate from the degradation, diagenesis, and catagenesis of fossil biological matter, so k_2 should be strictly positive. As the other biological compounds of embalming materials are much more recent than bitumen, they may or may not contain radicals, so that $k_3 \geq 0$.

From eq 1, the EPR intensity of radicals is related to that of VO-P by

$$I_{C^0} = \left(\frac{k_2 - k_3}{k_1}\right) I_{VO-P} + k_3 \quad (2)$$

https://dx.doi.org/10.1021/acs.analchem.0c03116
Anal. Chem. XXXX, XXX, XXX−XXX

Except the reference sample ***TS***, all of the experimental data lie in the surface limited by the lines $I_C0 \approx 3 \times I_{VO\text{-}P}$ (full line) and $I_C0 \approx 5 \times I_{VO\text{-}P}$ (dashed line). Several pieces of information can be deduced from these results:

(i) These two lines intercept the origin, which corresponds to $k_3 \approx 0$ and indicates that radicals C^0 are almost exclusively localized in the bitumen component of the balm.

(ii) The fact that the ratios k_2/k_1 in historical and reference samples (except ***TS***) lie in a narrow range of values, $3 \leq k_2/k_1 \leq 5$, shows that the bitumen originates from vanadium-rich sources, possibly the same, in all cases. This could indicate that the bitumen of historical samples originates from floating blocks in the north part of the Dead Sea (vanadium rich) rather than from the south part (vanadium poor).[10]

(iii) The commercial bitumen of Judea (***Ref 2***) is characterized by a higher ratio, $k_2/k_1 \approx 5$, than the Dead Sea asphalt ***Ref 1*** ($k_2/k_1 \approx 3$), which can be due to a different geological setting for the source of ***Ref 2*** (slightly depleted in VO-P) or to the chemical treatment used for obtaining the brown powder.

(iv) Again, the data points of ***Hum 3*** and ***Ref 2*** are very close in the diagram.

Two hypotheses may be proposed to explain the similitude of these two data in two independent diagrams (Figure 5a,b): (a) the bitumen samples of ***Ref 2*** and ***Hum 3*** come from the same geological setting and (b) the mummy ***Hum 3*** has been partially restored with bitumen of Judea. Hypothesis b) is reinforced by the fact that ***Hum 3***, unlike the other historical samples, contains no VO-nP complexes and is very rich in bitumen. This hypothesis is discussed in the last section of this article.

Out-of-Phase EPR. X-band EPR spectra of historical samples (Figures 3b, S1, and S2) contain four types of overlapping spectra, i.e., free radicals C^0, complexes VO-P and VO-nP, and traces of ferromagnetic particles. In the absence of simulation, such crowded spectra can be difficult to interpret. However, when paramagnetic species differ by their spin-lattice relaxation times T_1, it is possible to improve the spectral selectivity by playing with the phase shift of the detected signal. In cw-EPR, the static magnetic field is harmonically modulated, generally at the frequency $\omega_m/2\pi$ = 100 kHz in standard spectrometers. The response of the spin system to the resulting modulation of the Zeeman interaction is phase-shifted relative to the modulated field.[28] Two components of the EPR signal can be detected: the in-phase and the out-of-phase components with respect to the static field modulation. The in-phase detection is routinely used in standard EPR as it gives all of the EPR signals present in the sample. The out-of-phase signal is sensitive to phase retardation effects, so that it is sensitive only to EPR signals with long spin-lattice relaxation times T_1.[29] EPR signals with short T_1 do not give the out-of-phase signal. Both in-phase and out-of-phase spectra were recorded at a microwave power of 2 mW, which correspond to the optimal intensity of the out-of-phase intensity relative to the in-phase intensity. Figure 6 shows an example of the EPR spectrum at the X-band for ***Hum 1***, recorded in-phase and out-of-phase with the modulation. The in-phase spectrum is the superposition of four different signals: the vanadyl complexes VO-P and VO-nP (marked by green circles), free radicals C^0, and the broad line (iron oxide particles) distorting the baseline.

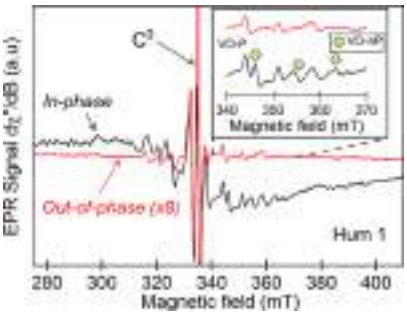

Figure 6. EPR spectra at room temperature of ***Hum 1*** recorded in-phase (black) and out-of-phase (red) with respect to the modulation.

The out-of-phase spectrum contains only the VO-P and C^0 signals. This shows that these two species have longer T_1 than the VO-nP complex. In-phase and out-of-phase spectra of other samples are given in the Supporting Information (Figure S4).

The amplitudes of the EPR lines of the out-of-phase signal (denoted I') versus the in-phase signal (denoted I) are shown in Figure 7a for C^0 and in Figure 7b for the $-1/2 \perp$ transition

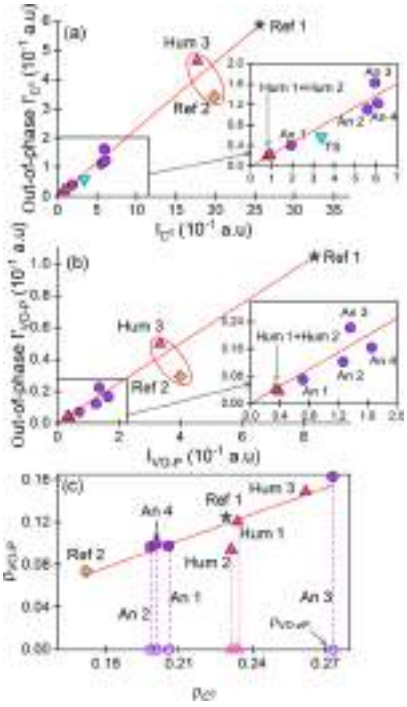

Figure 7. Out-of-phase versus in-phase EPR amplitude for (a) radicals C^0 and (b) VO-P complex; (c) diagram showing the correlation between the ratios $\rho = I'/I$ of VO-P and C^0.

of VO-P complexes. All of the experimental points are roughly placed along lines with slopes 0.23 for radicals and 0.12 for VO-P, and they are nearly superimposed in the case of ***Hum 1*** and ***Hum 2***. Again, these diagrams show the relative proximity of ***Hum 3*** and ***Ref 2***. As the out-of-phase signal is very sensitive to relaxation times T_1,[29] these almost linear relations between I' and I for C^0 and VO-P signals show that all of the samples studied contain the same types of free radicals and VO-P complexes with the same chemical environment (which control T_1). Indeed, if some samples had contained species (radicals or complexes) with long T_1 and other species with

https://dx.doi.org/10.1021/acs.analchem.0c03116
Anal. Chem. XXXX, XXX, XXX−XXX

short T_1, only those with long T_1 would give out-of-phase signals. In such a situation, one would expect data scattered throughout the diagram.

It is interesting to note that the out-of-phase behavior of the C^0 line in bitumen ***TS*** (Clermont-Ferrand, France) is the same as that of C^0 in all samples (Figure 7a). This shows that the C^0 radicals have the same T_1 in all types of bitumen. For the sake of interpreting these results, let us consider the ratio $\rho = I'/I$ of the out-of-phase to in-phase signal amplitudes. Figure 7c represents the variation of ρ for VO-P (denoted $\rho_{VO\text{-}P}$) versus ρ for C^0 (denoted ρ_C0) for all of the samples. The data appear linearly correlated with $\rho_{VO\text{-}P} \approx 0.83\rho_{C0}$, which is the indication of a simple relation between relaxation times of VO-P and C^0 for all of the samples.

The theory of out-of-phase EPR signals is rather complex;[29,30] however, under reasonable assumptions, ρ can be expressed as[31]

$$\rho \propto \omega_m T_1 \frac{s}{1+s} \tag{3}$$

where $s = \gamma_e^2 B_1^2 T_1 T_2$ is the saturation factor, with T_1 and $T_2 < T_1$ the spin-lattice and spin−spin relaxation times, respectively; γ_e is the electron gyromagnetic ratio; and B_1 is the amplitude of the microwave field. Relaxation measurements in various asphaltene samples by Mamin et al.[32] showed that relaxation times T_2 of radicals and VO-P are linked by the relation $T_2^{VO\text{-}P} \approx 0.43 \times T_2^{C^0}$. By fixing the experimental conditions, i.e. ω_m and the microwave power $P \propto (B_1)^2$, and under low saturation conditions ($s < 1$), which is the case with the present experiments, the ratio ρ for VO-P and C^0 is linked by the following relationship deduced from expression 3

$$\rho_{VO-P} \approx \left(\frac{T_1^{VO-P}}{T_1^{C^0}}\right)^2 \frac{T_2^{VO-P}}{T_2^{C^0}} \rho_{C^0} \approx 0.43 \left(\frac{T_1^{VO-P}}{T_1^{C^0}}\right)^2 \rho_{C^0} \tag{4}$$

From the slope of the curve in Figure 7c and from eq 4, we can deduce that T_1 values of VO-P and radicals are nearly equal, $T_1^{VO\text{-}P} \approx 1.4 \times T_1^{C^0}$, in all samples. As T_1 depends not only on the nature of paramagnetic species but also on their chemical environment, this nearly constant ratio between T_1 values of VO-P and C^0 indicates that their T_1 values are correlated. It is known that VO-P and C^0 are mainly located in the asphaltene component in oil and bitumen.[17,32] Direct relaxation measurements by pulsed-EPR on a series of asphaltene samples showed that the distance between C^0 and VO-P does not exceed a few nanometers, which results in a correlation between their T_1.[32] The closeness of T_1 in VO-P and C^0 in all samples studied in this work indicated that this weak VO-P−C^0 interaction was conserved in black matter of all animal and human mummies and was not affected by the preparation of the embalming matter.

On the contrary, VO-nP complexes, which are found only in historical samples (except ***Hum 3***), are systematically characterized by $\rho_{VO\text{-}nP} = 0$ (Figure 7c), showing that their T_1 is very small, $T_1^{VO\text{-}nP} \ll T_1^{VO\text{-}P}$ and $T_1^{VO\text{-}nP} \ll T_1^{C^0}$. These inequalities suggest that the oxygenated VO-nP complexes originate from the extraction of VO^{2+} from VO-P complexes in an asphaltene environment and their complexation by oxygenated ligands in a different environment.

Paramagnetic markers of bitumen and authentication of the black matter in Egyptian mummies. VO-P complexes and carbonaceous radicals C^0 are stable markers of oil and bitumen,[10−12] and their detection by EPR in a black matter with complex composition is a direct and nondestructive method to reveal, without ambiguity, the presence of bitumen in its composition (Figure 4b). These markers are mainly localized in the asphaltene component of bitumen, which is the most resistant component to biodegradation and oxidation.[13] C^0 and VO-P are spatially connected in asphaltene, which manifests by a correlation between their relaxation times.[32] Using a combination of in-phase and out-of-phase detection, we observed such a correlation between relaxation times, which demonstrate that the nanostructuration of VO-P and C^0 is conserved in bitumen of historical samples (Figure 7). This result strongly suggests that bitumen was not chemically and/or biologically modified during the preparation of the embalming matter and after burial of the mummy.

Historical samples (except ***Hum 3***) contain also nonporphyrinic VO-nP complexes, where VO^{2+} ions have four oxygen ligands. Contrary to VO-P, these VO-nP complexes are not associated with carbonaceous radicals C^0 of the bitumen (their relaxation times T_1 are not correlated). Three possible origins can be proposed for the presence, in the embalming black matter, of such oxygenated vanadyl complexes: (i) first, VO-nP could originate from weathering alteration at ambient temperature over thousands of years after burial; (ii) second, they could be the result of biodegradation by bacteria, insects, or fungi present in the mummy; and (iii) third, VO-nP could originate from reaction of VO-P with carboxylate functions of other biological compounds of the balm mixture. At first sight, mechanism (i) is probably not predominant as such VO-nP complexes have not been observed in extensively weathered tar ball coming from the 2010 Deepwater Horizon oil spill in the Gulf of Mexico,[33] which indicates that even an intense weathering is not sufficient to produce VO-nP complexes. Indeed, VO-P complexes are known to be very stable, and temperatures higher than 400 °C are required for their destruction.[10] The formation of VO-nP-type complexes in asphaltene is possible only by heating at 250 °C in air for several days.[34] Mechanisms (ii) and (iii) appear more reasonable. Mummies generally present evidence of alteration by microorganisms, insects, and fungi.[35,36] Also, it is known that microbial growth and biodegradation of oil spills are stimulated by trace metal elements.[37,38] As bitumen contains Ni and VO porphyrins, these complexes may be somewhat modified by the microbial activity. For example, peroxidase enzymes are known to produce a demetallation of petroporphyrins,[39] i.e., an extraction of VO^{2+} ions from VO-P, which may hereafter stabilize by forming oxygenated VO-nP complexes. Regarding mechanism (iii), we may also propose that VO^{2+} ions of VO-P located at the interface between bitumen and other biological components of the black matter (plant oil, tree resin, beeswax, animal fats, etc.) form VO...O bonds by complexation with carboxylate functions present in these agents (a schematic model is presented in Figure 8). A combination of mechanisms (ii) and (iii) could also be considered, in which microbial activity could result in the extraction of VO^{2+} ions from VO-P complexes, followed by their complexation by the oxygenated functions of other biomolecules of the black matter.

https://dx.doi.org/10.1021/acs.analchem.0c03116
Anal. Chem. XXXX, XXX, XXX−XXX

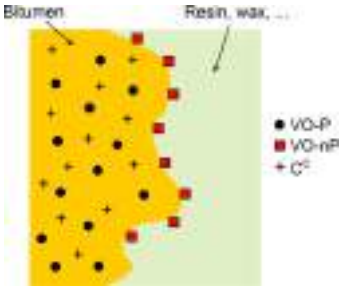

Figure 8. Schematic model showing the nonporphyrinic vanadyl complexes VO-nP at the interface between bitumen and the vegetal component of the embalming material.

Let us now consider the case of sample ***Hum* 3**, which was taken from the mummy found in Nehemsimontou's coffin (XXVth dynasty, 744−656 BC). The ensemble was purchased in 1837 from a private collector by the municipality of Boulogne, France. However, it later turned out that the mummy and the coffin had nothing in common and that they had been assembled for the purpose of a better sale, a common practice in the 19th century. It is the mummy of a bearded man with short, curly hair, about 1.69 m tall (Figure 1c). The body is coated with a solid, black, shiny substance, which drips in some places.[40] ***Hum* 3** was sampled from the neck of the mummy and has many EPR characteristics that make it different from the other historical samples investigated in this work: (i) a high abundance of VO-P, suggesting that it is pure (or almost pure) bitumen (Figure 4b), as also demonstrated by GC/MS analysis (Supporting Information); (ii) the absence of VO-nP, an evolution marker found in all other historical samples (Figure 5a); (iii) a C^0/VO-P intensity ratio different from other historical samples and similar to that of a reference sample, the commercial bitumen of Judea ***Ref* 2** (Figure 5b). All of these features suggest that the mummy was covered with bitumen, which has not been altered by subsequent chemical or biological reactions. As also supported by molecular data, we must thus consider the possibility that this mummy was restored with pure bitumen before it was acquired by the museum of Boulogne in 1837.

CONCLUSIONS AND PERSPECTIVE

EPR of vanadyl complexes and carbonaceous radicals of asphaltene is a nondestructive tool to study embalming materials in ancient Egypt. As VO-P complexes are ubiquitous in petroleum, asphalt, and bituminous rocks of marine origin in all continents and in geological formations with a wide range of age, their detection in archeological balms unambiguously indicates the presence of bitumen in this material. Also, carbonaceous radicals are present in all kerogeneous materials and originate from the maturation of biomolecules during tens to hundreds of million years of geological evolution. They are also present in asphaltene of all bitumen samples, whether or not of the marine origin.[41] These radicals are absent in more recent biological materials, so that the presence of both VO-P and radicals in the complex mixture of embalming materials is a very sensitive marker of the presence of a bitumen component in this black material. An advantage of standard cw-EPR at the X-band is the fact that a millimeter-size sample can be studied without any chemical preparation. As the bitumen content in balms is generally underestimated by the molecular analysis approach currently used in most archeometric studies,[42] EPR is a rapid and sensitive complementary method to detect bitumen. Even in the case of complex EPR spectra containing overlapping signals of different nature, VO-P and carbonaceous radicals can be selectively detected using the out-of-phase detection mode of the EPR signal. This approach is new to the best of our knowledge.

Other conclusions of this work are summarized as follows: (i) VO-P and C^0 markers of bitumen are well protected against biodegradation and atmospheric degradation in the highly polymerized asphaltene component of bitumen. (ii) The conservation, in historical samples, of the nanostructuration of VO-P and C^0 radicals in the bitumen component of balms (revealed by the correlation between their relaxation times T_1) indicates that the natural bitumen (most probably taken from the Dead Sea) was not affected by the mixture with other embalming agents. (iii) The black matter sampled from mummies and coffin also contains nonporphyrinic vanadyl VO-nP complexes with oxygenated ligands replacing the nitrogen ligands of the porphyrin ring. They probably originate from the biological and/or chemical reaction of VO-P with carboxylate functions of the vegetal or animal components of the balm. (iv) One sample taken from a human mummy does not contain this VO-nP marker and is made of pure unaltered bitumen. This suggests that this mummy could have been partially restored in the early 19th century.

Although more quantitative analyses of these markers are needed for eventual dating and authentication applications, the absence of VO-nP could be used to detect any undocumented restoration of mummies with bitumen. This may be useful for the analysis of objects containing dark matter, once acquired by museums through donations or purchases from private collectors in the 19th century, at a time when many excavations of archeological sites often resembled pillaging. Also, although most of the bitumen used in mummies or their wooden coffins came from the Dead Sea area in Palestine,[1,21,43−45] it is necessary to compare historical bitumen with bitumen from other sources, for example, Gebel El Zeit, Gulf of Suez, that have sometimes been used by ancient Egyptians.[20,46]

For future research, a detailed analysis of the structure and surrounding of vanadyl complexes (porphyrinic and nonporphyrinic) and radicals by more sophisticated EPR techniques would provide clues to the fabrication receipts and the evolution/degradation of embalming materials. First, electron nuclear double resonance (ENDOR) spectroscopy will provide additional information on the evolution of VO-P complexes by probing hyperfine interactions with ^{1}H nuclei of metallic complexes and radicals.[47] Second, pulse-EPR methods will allow direct measurements of relaxation times T_1 and T_2 and measurement of small hyperfine interactions with ^{14}N, ^{13}C, ^{31}P, and ^{33}S nuclei.[17,32,48] However, the ease of use of standard continuous-wave X-band EPR spectroscopy (recording a spectrum takes only a few minutes) and the ubiquity of vanadyl geoporphyrins VO-P and radicals in bitumen open the door to the easy characterization of bitumen in all types of archeological artifacts. Our novel approach can be complementary to another recent relevant study.[49]

ASSOCIATED CONTENT

Supporting Information

The Supporting Information is available free of charge at https://pubs.acs.org/doi/10.1021/acs.analchem.0c03116.

https://dx.doi.org/10.1021/acs.analchem.0c03116
Anal. Chem. XXXX, XXX, XXX−XXX

Description of samples; EPR spectra of references and historical samples; EPR spectrum of the *TS* sample; in-phase and out-of-phase EPR spectra; simulation parameters; and sample preparation and GC/MS analyses (PDF)

AUTHOR INFORMATION

Corresponding Authors

Charles E. Dutoit − *Chimie-ParisTech, PSL University, CNRS, Institut de Recherche de Chimie-Paris (IRCP), F-75005 Paris, France*; Email: Charles.dutoit@chimieparistech.psl.eu

Didier Gourier − *Chimie-ParisTech, PSL University, CNRS, Institut de Recherche de Chimie-Paris (IRCP), F-75005 Paris, France*; orcid.org/0000-0002-9996-9297; Email: didier.gourier@chimieparistech.psl.eu

Authors

Laurent Binet − *Chimie-ParisTech, PSL University, CNRS, Institut de Recherche de Chimie-Paris (IRCP), F-75005 Paris, France*

Hitomi Fujii − *Centre de Recherche et de Restauration des Musées de France (C2RMF), F-75001 Paris, France*

Agnes Lattuati-Derieux − *Centre de Recherche et de Restauration des Musées de France (C2RMF), F-75001 Paris, France*

Complete contact information is available at: https://pubs.acs.org/10.1021/acs.analchem.0c03116

Author Contributions

C.E.D., L.B., and D.G. performed and interpreted EPR measurements. H.F. and A.L.-D. analyzed the samples by GC/MS. The manuscript was written by D.G. through contributions of all authors. All authors have given approval to the final version of the manuscript.

Notes

The authors declare no competing financial interest.

ACKNOWLEDGMENTS

C.E.D., D.G., and L.B. received funding from Agence Nationale de la Recherche (ANR) under contract No. ANR-17-CE29-0002-01. A.L. and H.F. received funding from the Centre de Recherche et de Restauration des Musées de France (C2RMF). We thank Aurélie Artizzu for providing information about some historical samples studied in this work. The authors are very grateful to the Musée Dobrée in Nantes, the Musée d'Art et d'Histoire in Narbonne, the Musée des Confluences in Lyon, the Chateau-Musée de Boulogne-sur-Mer and more especially to Julie Pellegrin, Camille Broucke, Flore Collette, Elikya Kandot, and Gaëlle Etesse who are in charge of collections. In addition, we would like to express our gratitude to Noëlle Timbart, curator at the C2RMF for her fruitful help, to Nathalie Balcar, conservation scientist at the C2RMF for the mummy samples and informative exchanges, and to Armelle Charrié for analytical data.

REFERENCES

(1) Maurer, J.; Möhring, T.; Rullkötter, J.; Nissenbaum, A. *J. Archaeol. Sci.* **2002**, *29*, 751−762.
(2) Buckley, S. A.; Clark, K. A.; Evershed, R. P. *Nature* **2004**, *43*, 294−298.
(3) Clark, K. A.; Ikram, S.; Evershed, R. P. *Philos. Trans. R. Soc., A* **2016**, *374*, No. 20160229.
(4) Granville, A. B. *Philos. Trans. R. Soc., A* **1825**, *4115*, 269−316.
(5) Lucas, A. *J. Egypt. Archaeol.* **1914**, *1*, 241−245.
(6) Spielmann, P. E. *J. Egypt. Archaeol.* **1933**, *18*, 177−180.
(7) Lucas, A.; Harris, J. R. *Ancient Egyptian Materials and Industries*, 4th ed.; Histories and Mysteries of Man: London, 1989; p 523.
(8) Buckley, S. A.; Evershed, R. *Nature* **2001**, *413*, 837−841.
(9) Breit, G. N.; Wanty, R. B. *Chem. Geol.* **1991**, *91*, 83−97.
(10) Premović, P. I.; Tonsa, I. R.; Pavlovic, M. S.; Lopez, L.; LoMonaco. *Fuel* **1998**, *77*, 1769−1776.
(11) Rullkötter, J.; Spiro, B.; Nissenbaum, A. *Geochim. Cosmochim. Acta* **1985**, *49*, 1357−1370.
(12) Baker, E. W.; Louda, J. W. *Biological Markers in the Sedimentary Record*; John, R. B., Ed.; Elsevier: Amsterdam, Netherlands, 1986; pp 125−225.
(13) Connan, J.; Zumberge, J.; Imbus, K.; Moghaddam, A. *Org. Geochem.* **2008**, *39*, 1772−1789.
(14) Stoll, S.; Schweiger, A. *J. Magn. Reson.* **2006**, *178*, 42−55.
(15) Saraceno, A. J.; Coggeshall, N. D.; Fanale, D. T. *Anal. Chem.* **1961**, *33*, 500−505.
(16) Aizenshtat, Z.; Sundararaman. *Geochim. Cosmochim. Acta* **1989**, *53*, 3185−3188.
(17) Ben Tayeb, K.; Delpoux, O.; Barbier, J.; Marques, J.; Verstraete, J.; Vezin, H. *Energy Fuels* **2015**, *29*, 4608−4615.
(18) Goodman, B. A.; Raynor, J. B. Electron Spin Resonance of Transition Metal Complexes. In *Advances in Inorganic Chemistry and Radiochemistry*; Emeleus, H. J.; Sharpe, A. G., Eds.; Academic Press: New York, 1970.
(19) Gourier, D.; Delpoux, O.; Bonduelle, A.; Binet, L.; Ciofini, I.; Vezin, H. *J. Phys. Chem. B* **2010**, *114*, 3714−3725.
(20) Harrell, J. A.; Lewan, M. D. *Archaeometry* **2002**, *44*, 285−293.
(21) Nissenbaum, A.; Buckley, S. *Archaeometry* **2013**, *55*, 563−568.
(22) Connan, J.; Van de Velde, T. *Arabian Archaeol. Epigr.* **2010**, *21*, 1−19.
(23) Nissenbaum, A. *Rev. Chem. Eng.* **1993**, *9*, 365−383.
(24) Skrypczak-Bonduelle, A.; Binet, L.; Delpoux, O.; Vezin, H.; Derenne, S.; Robert, F.; Gourier, D. *Appl. Magn. Reson.* **2008**, *33*, 371−397.
(25) Bourbin, M.; Gourier, D.; Derenne, S.; Binet, L.; Le Du, Y.; Westall, F.; Kremer, B.; Gautret, P. *Astrobiology* **2013**, *13*, 151−162.
(26) Binet, L.; Gourier, D.; Derenne, S.; Robert, F. *Geochim. Cosmochim. Acta* **2002**, *66*, 4177−4186.
(27) Gourier, D.; Binet, L.; Calligaro, T.; Capelli, S.; Vezin, H.; Bréhéret, J.; Hickman-Lewis, K.; Gautret, P.; Campbell, K.; Westall, F. *Geochim. Cosmochim. Acta* **2019**, *258*, 207−225.
(28) Abragam, A.*The Principles of Nuclear Magnetism*; Marshall, W. C.; Wilkinson, D. H.; Eds; Oxford University Press: Oxford, 1961.
(29) Livshits, V. A.; Pali, T.; Marsh, D. *J. Magn. Reson.* **1998**, *134*, 113−123.
(30) Kälin, M.; Gromov, I.; Schweiger. *J. Magn. Reson.* **2003**, *160*, 166−182.
(31) Livshits, V. A.; Marsh, D. *J. Magn. Reson.* **2005**, *175*, 317−329.
(32) Mamin, G. V.; Gafurov, M. R.; Yusupov, R. V.; Gracheva, I. N.; Ganeeva, Yu.M.; Yusupova, T. N.; Orlinskii, S. B. *Energy Fuels* **2016**, *30*, 6942−6946.
(33) Ramachandran, V.; van Tol, J.; McKenna, A. M.; Rodgers, R. P.; Marshall, A. G.; Dalal, N. S. *Anal. Chem.* **2015**, *87*, 2306−2313.
(34) Premović, P. I.; Tonsa, I. R.; Pajovic, M. T.; Lopez, L.; Monaco, S. L.; Dordevic, D. M.; Pavlovic, M. S. *Fuel* **2001**, *80*, 635−639.
(35) Gülaçara, F. O.; Susini, A.; Klohn, M. *J. Archaeol. Sci.* **1990**, *17*, 691−705.
(36) Arya, A.; Shah, A. R.; Sadasivan, S. *Curr. Sci.* **2001**, *7*, 793−799.
(37) Dedeles, G. R.; Abe, A.; Saito, K.; Asano, K.; Saito, K.; Yokota, A.; Tomita, F. *J. Biosci. Bioeng.* **2000**, *90*, 515−521.
(38) Mejeha, O. K.; Head, I. M.; Sherry, A.; McCann, C. M.; Leary, P.; Jones, D. M.; Gray, N. D. *Chemosphere* **2019**, *237*, No. 124545.
(39) Fedorak, P. M.; Semple, K. M.; Vazquez-Duhalt, R.; Westlake, D. W. S. *Enzyme Microb. Technol.* **1993**, *15*, 429−437.
(40) Vincent, F. *Intervention concernant la momie d'homme, Château-Musée de Boulogne-sur-Mer*; C2RMF Report no. 6307, 2004.

(41) Zhang, Y.; Siskin, M.; Gray, M. R.; Walters, C. C.; Rodgers, R. P. *Energy Fuels* **2020**, *34*, 9094−9107.
(42) Lucejko, J.; Connan, J.; Orsini, S.; Ribechini, E.; Modugno, F. *J. Archaeol. Sci.* **2017**, *85*, 1−12.
(43) Rullkötter, J.; Nissenbaum, A. *Naturwissenschaften* **1988**, *75*, 618−621.
(44) Connan, J.; Dessort, D. *C. R. Seances Acad. Sci., Ser. 2* **1991**, *312*, 1445−1452.
(45) Connan, J.; Nissenbaum, A.; Dessort, D. *Geochim. Cosmochim. Acta* **1992**, *56*, 2743−2759.
(46) Barakat, A. O.; Mostafa, A.; Qian, Y.; Kim, M.; Kennikut, M. C., II *Geoarcheology* **2005**, *20*, 211−228.
(47) Mannikko, D.; Stoll, S. *Energy Fuels* **2019**, *33*, 4237−4243.
(48) Biktagirov, T.; Gafurov, M.; Mamin, G.; Gracheva, I.; Galukhin, A.; Orlinskii, S. *Energy Fuels* **2017**, *31*, 1243−1249.
(49) Fulcher, K.; Stacey, R.; Spencer, N. *Sci. Rep.* **2020**, *10*, No. 8309.

https://dx.doi.org/10.1021/acs.analchem.0c03116
Anal. Chem. XXXX, XXX, XXX−XXX